Optimizing for Spatial Frequency Coverage vs. Point-Spread Function Sidelobe Level in Active Incoherent Microwave Imaging Arrays

Sean Ellison, Stavros Vakalis, and Jeffrey A. Nanzer
Electrical and Computer Engineering, Michigan State University, East Lansing, MI, USA
{elliso65, vakaliss, nanzer}@msu.edu

***Abstract*—Array optimization to maximize image reconstruction performance is often approached using numerical methods due to the solution space being too large for traditional brute force methods. In this work, a sixteen platform coherent distributed array with a seven element subarray attached to each platform will be optimized in two separate domains, each using a genetic algorithm: one to optimize spatial frequency content and the other to optimize peak to sidelobe level of the point spread function. The dimension of the array solution space is restricted to a planar domain of $50\lambda \times 50\lambda$, and the image reconstruction performance is compared for the outputs of both optimization approaches. It is demonstrated that optimizing the point spread function results in better reconstruction of images containing typical spatial frequency distributions, while optimizing the spatial frequency coverage results in better reconstruction of images containing mostly high-spatial frequency content, such as images consisting mostly of shape outlines.**

I. Introduction

Correlator antenna arrays have been around for decades and have had a significant impact in the field of interferometry [1]; more recently, the authors developed a new form of microwave imaging based on active incoherent interferometry [2]. The dimensions of the correlator arrays allow for a spatial-filtering behavior and therefore the spatial frequency content of an array can be found from the unique pairwise correlated output signals form all antenna elements. To obtain the clearest image possible from a distant source, the maximum coverage in the spatial frequency domain ($u - v$ domain) or minimum sidelobes in the the angular domain ($l - m$ domain) is needed. Due to the extremely large number of formations that arrays can take in a planar domain, numerical optimization is often used to approach such problems [3], [4] . While these and other works typically consider specific formations (e.g. T- or Y-shaped), this work explores element locations in a planar domain. Image formation results are compared between optimizing the array for maximized spatial frequency coverage and minimized sidelobe level on the point-spread function. Two types of images are compared: one with typical spatial frequency content, and one consisting of primarily high-spatial frequency content, which is represented largely in the edges of shapes.

II. Incoherent Imaging Array

The array considered in this work consists of sixteen nodes placed randomly in a $50\lambda \times 50\lambda$ planar domain using a uniformly distributed random number generator. Each node has a seven element subarray with spacing 0.5λ, 1λ, and 2λ in an L-shaped pattern. An image of the subarray layout can be seen in Fig. 1. The subarray ensures that low spatial frequencies are always represented in the array, thus the optimization more heavily weights node locations that maximize high spatial frequency content.

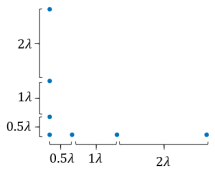

Fig. 1: Subarray on each platform.

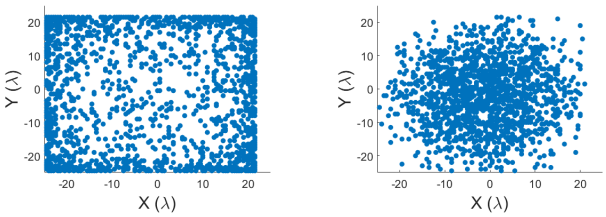

Fig. 2: (a) Converged solutions when optimizing in the spatial frequency domain (b) Converged solutions when optimizing in the angular domain.

The optimization technique that is used is a genetic algorithm that optimizes the locations of each node. The fitness function optimizing for the spatial frequency content is the percent coverage of the spatial frequency domain and peak to sidelobe level for optimizing the point spread function. The stop criterion is set to be 100 generations. This process is run for 100 Monte Carlo iterations. The density of the converged outputs can be seen in Fig. 2. It can be seen that when optimizing for the spatial frequency content that the solutions tend cluster to the outside of the domain with an average coverage of 23.4% in the spatial frequency domain. This is to be expected because it will maximize the total number of unique pairwise connections that can be made and as a result maximizes the coverage in the spatial frequency domain. It can

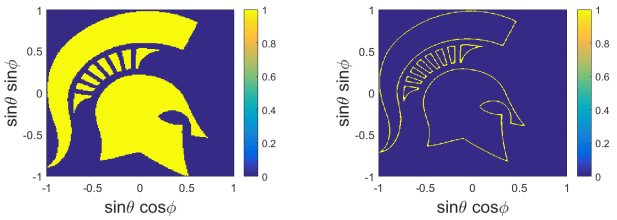

Fig. 3: Image of Spartan helmet with (a) typical spatial frequency content and (b) high spatial frequency content.

also be seen that when optimizing for the peak to sidelobe level in the angular domain, solutions tend to cluster to the middle of the solution space resulting in an average sidelobe suppression of 11.45 dB. This is to be expected since higher levels of sparsity result in a larger number of sidelobes.

III. Optimization and Image Formation Results

Since both of these optimized formations are used for imaging, the performance will be assessed by reconstructing an image of the Michigan State University Spartan helmet in Fig. 3. The image (a) is to assess overall image reconstruction ability and the image (b) is to assess the ability to reconstruct high spatial frequency content. For the optimized spatial frequency domain the reconstruction takes place through multiplication with the Fourier transform of the scene and for the sidelobe suppression the image formation takes place with a convolution between the scene and the point spread function in the angular domain. This is done so that the image is recreated using the respective optimized domains. An example of a layout found from optimizing for spatial frequency coverage can be seen in Fig. 4 along with the resulting image. This layout achieved 23.75% coverage and in turn a peak-to-sidelobe level of 7.85 dB. An example of a layout found from optimizing for the point spread function can be seen in Fig. 5 along with the resulting image. This layout achieved a peak-to-sidelobe level of 11.59 dB and a 15.26% coverage in spatial frequency domain.

To evaluate the average error created when doing this imaging technique, the resulting array formation reconstructions are compared to that of an ideal case (i.e. a completely filled spatial frequency domain). Reproducing the image in Fig. 3(a) the average mean squared error over 100 Monte Carlo iterations was 17.82% and 20.93% for sidelobe optimization and spatial frequency optimization, respectively. When producing the image in Fig. 3 (b) the average mean squared error was 2.98% and 15.84% for spatial frequency optimization and sidelobe suppression optimization respectively. This indicates that minimizing the sidelobes of the point-spread function will result in a more accurate image reconstruction for images with broad-spectrum spatial frequency content, but in images containing mostly higher spatial frequency content (i.e. edges), optimization of the spatial frequency sampling function results in better performance.

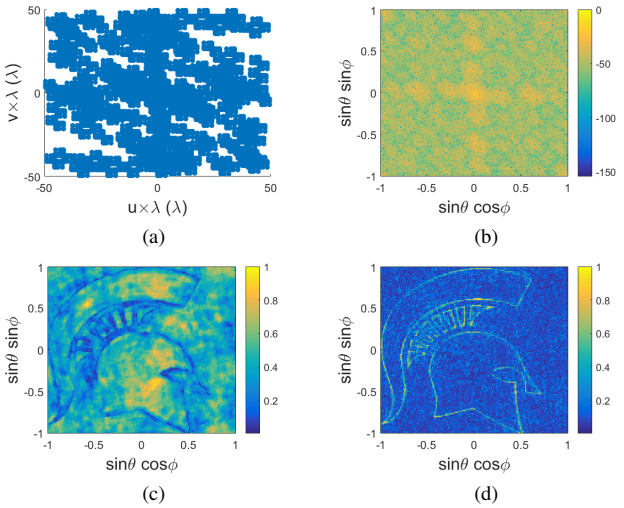

Fig. 4: (a) Node locations for optimization in spatial frequency domain (b) Spatial frequency content (c) Reconstructed image with typical spatial frequency content (d) Reconstructed image with high spatial frequency content

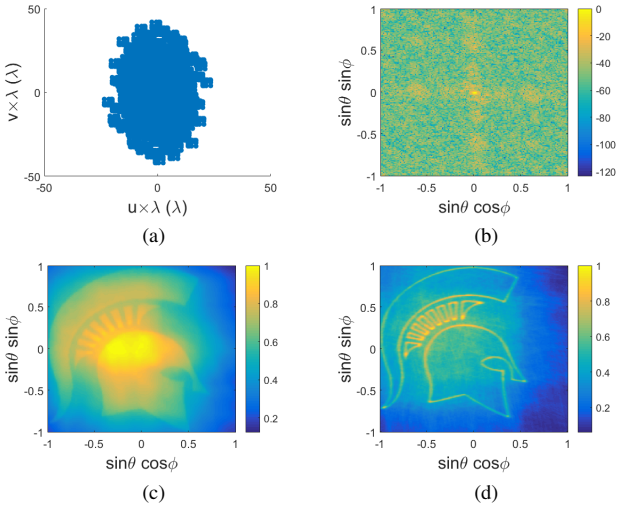

Fig. 5: (a) Node locations for optimization for peak to sidelobe level (b) Spatial frequency content (c) Reconstructed image with typical spatial frequency content (d) Reconstructed image with high spatial frequency content

References

[1] G. S. A. Thompson, J. Moran, *Interferometry and Synthesis in Radio Astronomy*, 3rd ed. John Wiley and Sons, 2001.

[2] S. Vakalis and J. A. Nanzer, "Microwave imaging using noise signals," *IEEE Trans. Microw. Theory Tech.*, vol. 66, no. 12, pp. 5842–5851, Dec 2018.

[3] K. Chao, Z. Zhao, Z. Wu, and R. Lang, "Application of the differential evolution algorithm to the optimization of two-dimensional synthetic aperture microwave radiometer circle array," in *2010 International Conference on Microwave and Millimeter Wave Technology*, May 2010, pp. 1212–1215.

[4] N. Jin and Y. Rahmat-Samii, "Analysis and particle swarm optimization of correlator antenna arrays for radio astronomy applications," *IEEE Trans. Antennas Propag.*, vol. 56, no. 5, pp. 1269–1279, May 2008.